Eur. Phys. J. B **53**, 5–9 (2006)
DOI: 10.1140/epjb/e2006-00349-8

THE EUROPEAN PHYSICAL JOURNAL B

Transport and magnetic properties of $Pr_{1-x}Ca_xCrO_3$ ($x = 0.0$–0.5): effect of t_{2g} orbital degeneracy on the thermoelectric power

S. Pal, S. Hébert[a], C. Yaicle, C. Martin, and A. Maignan

Laboratoire CRISMAT, UMR 6508 CNRS ENSICAEN, 6 bd Maréchal Juin, 14050 Caen Cedex 4, France

Received 19 May 2006 / Received in final form 27 July 2006

Abstract. We report on the resistivity (ρ), thermoelectric power (S for Seebeck) and magnetic measurements of the series $Pr_{1-x}Ca_xCrO_3$ ($x = 0.0$–0.5). These orthochromites exhibit a T independent, large and positive S, from 100 K to 700 K which follows the Cr^{4+} concentration. Upon Ca^{2+} for Pr^{3+} substitution, a concomitant decrease of the resistivity and S values is found. The evolution of S as a function of hole concentration (Cr^{4+}) can be nicely fitted by the modified Heikes formula which takes into account the orbital degeneracy associated to Cr^{3+}/Cr^{4+}. This is in good agreement with the model previously calculated by Marsh and Parris, in the case of weak magnetic coupling [Phys. Rev. B **54**, 7720 (1996)]. The magnetic susceptibility measurements support the assumption of a weak magnetic coupling since the antiferromagnetic ordering T_N values are found to be lower than 250 K. For $Pr_{0.7}Ca_{0.3}CrO_3$, the power factor $PF = S^2/\rho$ measured at 700 K is equal to 1.9×10^{-4} W m^{-1} K^{-2}. The present system, chemically stable in air up to $T > 1000$ °C, is promising for thermoelectric application at very high temperature.

PACS. 71.27.+a Strongly correlated electron systems; heavy fermions – 72.15.Jf Thermoelectric and thermomagnetic effects – 72.80.Ga Transition-metal compounds

1 Introduction

Theoretical study of thermopower in strongly correlated electron system has been done by several authors [1–5] based on the Hubbard model. At high temperatures, the thermopower is mainly a measure of the entropy per carrier, and this calculation is known as the Heikes formula [6]. In many experimental thermoelectric power studies, thorough analysis has been performed to calculate the carrier concentration from the temperature independent formulas of Heikes [6] or Chaiken and Beni [1]. It has been observed in recent years that additional degeneracy associated with the states of carrier occupation has to be considered to explain the thermoelectric properties [7]. For example, in the case of mixed valent systems $M^{n+}/M^{(n+1)+}$, the entropy associated to spin degeneracy has to be considered [8]. In many transition metal oxides with perovskite structure, there is, in addition to this spin degeneracy, more than one energetically degenerate spatial orbital.In the multiband systems (for example doped rare earth manganites), the Hund's rule coupling and the energy-level splitting between orbitals affect the electronic structure, so that the study of the effect of spin and orbital degrees of freedom on the thermopower is complicated. The high thermoelectric power in $NaCo_2O_4$ has been explained considering spin and orbital degeneracies of Co ionic states [7]. Marsh and Parris [3] have derived a series of relations for the temperature independent thermoelectric power considering the orbital degeneracy of Cr ion. Their model gives good agreement with the experimental value of the Seebeck coefficient of $La_{1-x}Sr_xCrO_3$ ($x \leq 0.2$) in both the high and low temperature limit. The results indicate that in these orthochromites, the theoretical calculation predicts that the temperature independent thermoelectric power might result from the carrier concentration and orbital degeneracy of the Cr. To demonstrate the above idea, for larger x content, we have studied thermoelectric properties of $Pr_{1-x}Ca_xCrO_3$, with Ca^{+2} for Pr^{+3} substitution. In addition, other orthochromites like $Pr_{0.95}Sr_{0.05}CrO_3$ have been studied.

From the technological point of view, orthochromites have been widely studied as refractory conducting ceramics because of their low electrical conductivity, oxidation resistance and high melting point (>2400 °C). These properties have led to applications in high temperature furnace heating elements and interconnections in solid oxide fuel cells [9]. An important feature in these oxides is that the thermoelectric power is almost temperature independent up to very high temperatures and that the resistivity monotonically decreases with the increase of temperature. These properties demonstrate the possibilities of orthochromites to be used as high temperature thermoelectric materials.

---

[a] e-mail: `uebing@mpie-duesseldorf.mpg.de`

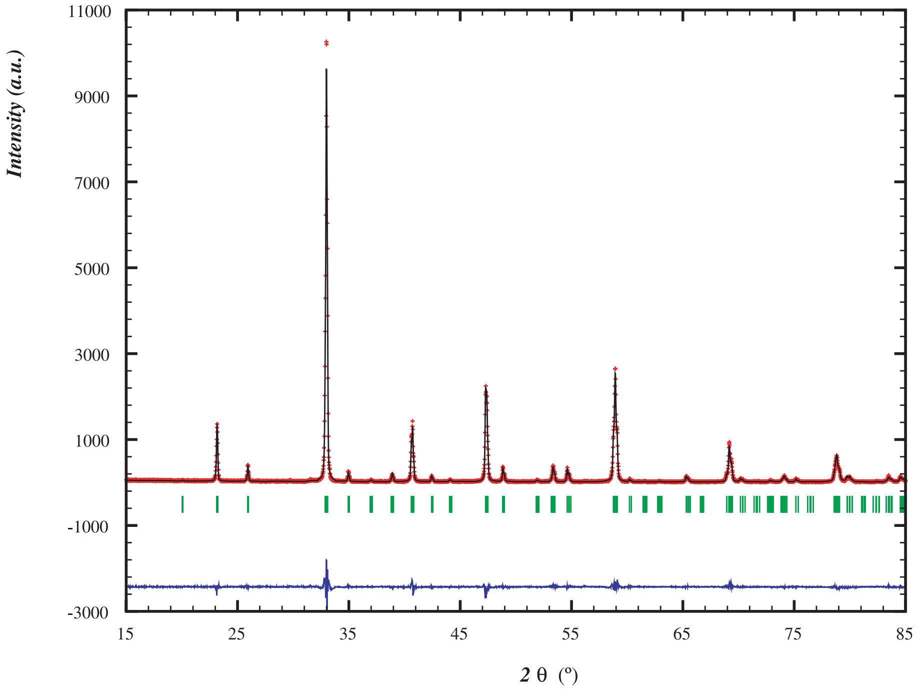

Fig. 1. The Rietveld refinement of the room temperature XRD data of $Pr_{0.8}Ca_{0.2}CrO_3$.

2 Experimental

A series of polycrystalline samples of compositions $Pr_{1-x}Ca_xCrO_3$ ($x = 0.0, 0.1, 0.2, 0.3$, 0.4 and 0.5) were prepared via solid state reaction method. The precursors Pr_6O_{11}, CaO and Cr_2O_3 were mixed in stoichiometric ratios. They were heated at 900 °C for 24 h. Then the powders were pelletized and fired in oxygen flow at 1200 °C for 12 h and 1500 °C for 24 h successively. The furnace was then cooled down to room temperature at a rate of 100 °C/h. $Pr_{0.95}Sr_{0.05}CrO_3$ has also been prepared in the similar way. The room temperature crystal structure was determined by powder X-ray diffraction (XRD) measurements using CuK_α radiation (Philips diffractometer). The lattice parameters were obtained from the Rietveld analysis of the XRD data using FULLPROF suite [10]. The resistivity data were collected using the four-probe technique. The Seebeck coefficient and thermal conductivity were measured simultaneously by using a steady-state method. A gradient of typically 1 K is installed through a small heater, and when the equilibrium is reached, two thermocouples measure the temperatures on the hot side and cold side, together with the gradient of voltage. The Seebeck coefficient S is directly equal to $\Delta V/\Delta T$, corrected from the contributions of the thermocouples, and the thermal conductivity is $\kappa = (RI^2 - A\sigma T^3 \Delta T_{up})/\Delta T$, where $R = 3.3$ kΩ is the resistance of the heater, ΔT_{up} the temperature on the hot side, σ the Stefan Boltzmann constant and A the surface of the sample sensitive to radiation. Quantum Design magnetometer was used to collect the ac susceptibility data. High temperature thermopower measurements have been performed up to 700 K by steady-state technique. High temperature resistivity has been measured using a standard four probe technique.

3 Results and discussion

The XRD patterns of the compounds $Pr_{1-x}Ca_xCrO_3$ (from $x = 0.0$ to 0.5) were refined in the orthorhombic perovskite $GdFeO_3$-type structure with Pnma or Pbnm space group [11]. The samples are single phases for $x < 0.4$, as shown in Figure 1 by the XRD pattern of the $x = 0.2$ compound. In the samples with $x = 0.4$ and 0.5, a second phase corresponding to $CaCrO_4$ is observed in small amount (<3%). The lattice parameters as well as the cell volume decrease with the Ca content. The similar ionic radius of Pr^{3+} (0.99 Å) and Ca^{2+} (1.00 Å) [12] cannot explain the lattice parameters decrease. Clearly, the introduction of Ca^{2+} is related to the creation of Cr^{4+} ion (0.55 Å) which has a smaller ionic radius than Cr^{3+}(0.615 Å).

In Figure 2, the thermal variation of electrical resistivity of $Pr_{1-x}Ca_xCrO_3$ with $0 \leq x \leq 0.30$ is shown. These samples are semiconducting-like ($d\rho/dT < 0$) throughout the temperature range of the measurements. Substitution of Ca^{2+} for Pr^{3+} ions creates holes in the t_{2g} orbitals (Cr^{3+} is a high spin cation, $3d^3$, $t_{2g}^3 e_g^0$) and thus, as x increases in $Pr_{1-x}Ca_xCr_{1-x}{}^{3+}Cr_x{}^{4+}O_3$, the p-type conductivity increases. As already reported [13], for this range of concentration, transport remains localized and can be explained by adiabatic hopping of small polarons, with $\sigma T \sim \exp(E/kT)$ (inset of Fig. 2). Grain boundaries effects can play a role in the resistive behaviour, but the small polaron hopping model is confirmed by the Seebeck coefficient, a technique less sensitive to the grain boundaries, and which is constant in the whole T range as shown in the following, as expected in this model.

The results of the temperature dependent thermopower measurements performed on these samples are

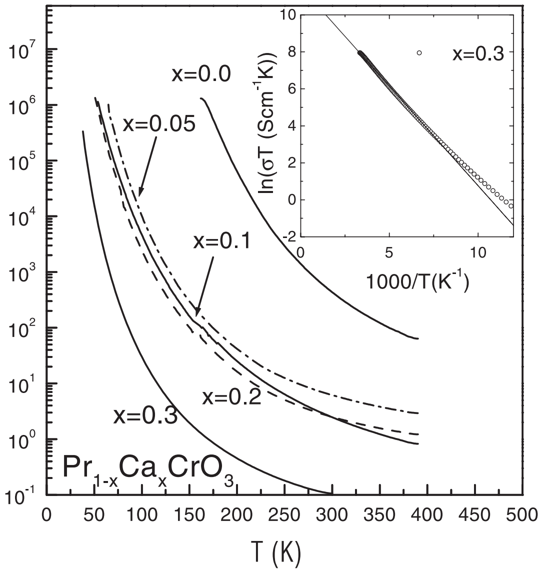

Fig. 2. Thermal dependence of the resistivity (ρ) for $Pr_{1-x}Ca_xCrO_3 (x = 0.0, 0.05, 0.1, 0.2, 0.3)$. Inset: $\ln(\sigma T)$ as a function of $1/T$ for $x = 0.3$.

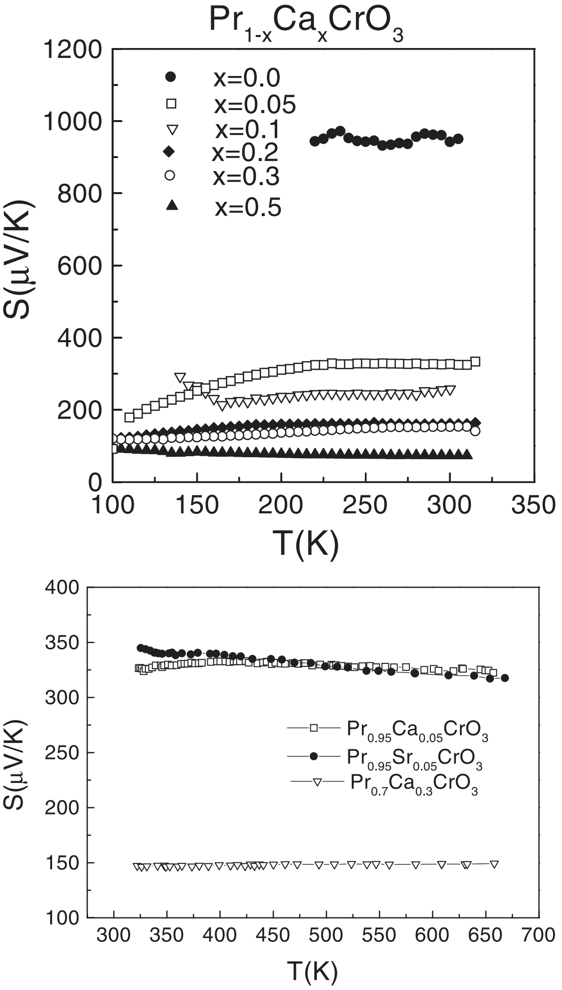

Fig. 3. (a) S vs. T plot of $Pr_{1-x}Ca_xCrO_3$ $(x = 0.0, 0.05, 0.1, 0.2, 0.3, 0.5)$. (b) High temperature (up to 650 K) data of some selected samples.

shown in Figure 3. For $PrCrO_3$ we have not been able to measure the thermopower below 200 K since the resistivity becomes very high ($>10^6$ Ω cm). All other samples have been measured down to ∼100 K. With the increase of the Ca content the Seebeck coefficient S decreases. Up to 300 K the S values are almost temperature independent for all the samples. To check the temperature dependence at higher temperatures, some selected samples have been also measured up to ∼700 K. Interestingly the S values remain almost constant up to the highest temperature of our measurement (Fig. 3b). This T independent value is characteristic of small polaron transport [13].

In Figure 4, thermal variation of the real part of the ac susceptibility (χ') is shown. The χ' value increases "monotonically" with decrease of temperature. A small anomaly is observed in all the samples below about 150–250 K and the temperature of the anomaly decreases with increase of Ca content. In $PrCrO_3$ this anomaly is observed around 236 K and may be assumed as the antiferromagnetic ordering temperature (T_N) of Cr^{3+} spins, in agreement with the value earlier reported [14, 15]. Susceptibility data of the samples follow a Curie-Weiss (CW) fit above T_N. Negative paramagnetic temperature Θ is obtained for all the compounds by extrapolating $(\chi')^{-1}$ to 0 (inset of Fig. 4). The exchange coupling between Cr^{3+} spins nearest neighbours in these compounds are predominantly antiferromagnetic. The antiferromagnetic ordering temperature (T_N) decreases with increase of Ca^{2+} substitution indicating the weakening of antiferromagnetic ordering between Cr^{3+} spins, as Cr^{4+} ions dilute the Cr^{3+}-O-Cr^{3+} superexchange interactions.

In Figure 5, the room temperature thermoelectric power $(S_{300\ K})$ has been plotted as a function of Ca content. The high temperature limit of the thermopower as a function of carrier density is given by the Heikes formula (solid line in Fig. 5) [6]:

$$S = k_B/e[\ln(1-x)/x]$$

where x is the concentration of charge carriers Cr^{+4} per available chromium site.

However, in the case of temperature-independent thermopower, the Heikes formula can be applied near room temperature also. By calculating the value of S for different x, it is observed that for each composition the experimental value $(S_{300\ K})$ is shifted up compared to the calculated value. Interestingly this shift is similar for all the compounds. A detailed calculation of the Seebeck coefficient in the $La_{1-x}Sr_xCrO_3$ orthochromites has been performed by Marsh and Parris [3]. Compared to the Heikes formula, S is shifted by ΔS_d, a value which depends on the spin and orbital degeneracies:

$$\Delta S_d = \frac{k_B}{e}\ln\left[\Gamma_{orb}\Gamma_{spin}\right]$$

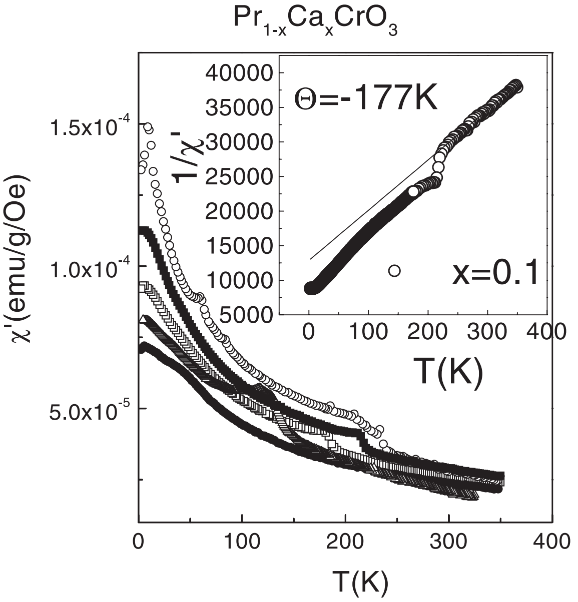

Fig. 4. Temperature dependent ac magnetic susceptibility of $Pr_{1-x}Ca_xCrO_3$: $x = 0.0$ (open circles), 0.1 (solid squares), 0.2 (open squares), 0.3 (solid circles). Inset: plot of reciprocal magnetic susceptibility vs temperature. Straight line corresponds to the Curie-Weiss fit.

with $\Gamma_{orb} = 3$ for Cr^{4+} ($3d^2$) and $\Gamma_{orb} = 1$ for Cr^{3+} ($3d^3$), and $\Gamma_{spin} = 2\sigma + 1$, where σ is the spin, in the case of weak magnetic coupling and $\Gamma_{spin} = 1$ for strong magnetic coupling. Remarkably, Figure 5 (dashed curve) shows that a good estimate of the Seebeck coefficients is obtained for $0 \leq x \leq 0.5$ in the case of weak magnetic coupling with

$$\Delta S_d = \frac{k_B}{e} \ln \left([\Gamma_{orb}\Gamma_{spin}]^{Cr^{4+}} / [\Gamma_{orb}\Gamma_{spin}]^{Cr^{3+}} \right)$$

$$= \frac{k_B}{e} \ln \left(\frac{3 \times 3}{1 \times 4} \right) = 69.9\ \mu V/K. \qquad (1)$$

Such a scenario is supported by the magnetic susceptibility data (Fig. 4) showing that in the present compounds the ordering temperatures occur below ~250 K. If one refers to the inverse magnetic susceptibility, above the ordering temperature, the samples are paramagnetic (linear regime) justifying a large spin degeneracy in this system.

To rule out a possible dependence on the ionic radius at the Pr^{3+}/Ca^{2+}-site, other orthochromites, $Pr_{1-x}Sr_xCrO_3$, have been prepared for Seebeck measurement purpose. For instance, the $Pr_{0.95}Sr_{0.05}CrO_3$ sample shows a T-independent S beyond RT. Accordingly, its room temperature S value is very close to the calculated curve of Figure 5. Clearly, the average ionic radius at the A-site of these ABO_3 perovskites has a much weaker effect upon S than the Cr^{3+}/Cr^{4+} mixed valency.

It is interesting to investigate the possibility of these oxides to be used as high temperature thermoelectric materials since the Seebeck coefficients are fairly large and temperature independent. The power factor, $PF = S^2/\rho$, evaluating the electrical components of the thermoelectric performance, shows that a low ρ value is also required for thermoelectric application. Figure 6 shows the resistivity of $Pr_{0.7}Ca_{0.3}CrO_3$ measured up to 700 K. At 650 K, ρ is close to 10^{-2} Ω cm and $S \sim 150\ \mu V/K$ which leads to a PF close to 1.9×10^{-4} W m^{-1} K^{-2}. A large number of oxides considered as good thermoelectrics for high temperature application exhibit similar PF values [16]. For comparison, the PF of polycrystalline $NaCo_2O_4$ is close to 8×10^{-4} W m^{-1} K^{-2} at 800 K [17]. Moreover, the present orthochromites, prepared by sintering in an oxygen flow at 1500 °C are chemically stable at least for temperature up to 1000 °C. All these facts suggest that the present oxides might be promising for thermoelectric application at very high temperature.

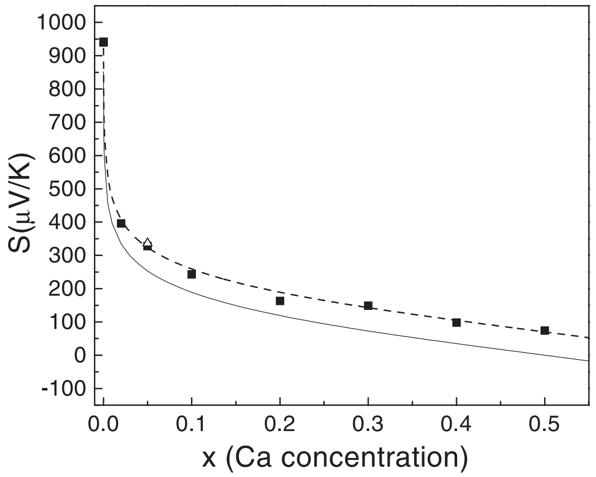

Fig. 5. Variation of room temperature S for $Pr_{1-x}Ca_xCrO_3$ (x= 0, 0.1, 0.2, 0.3, 0.4, 0.5), $Pr_{1-x}Sr_xCrO_3$ ($x = 0.05$). The solid curve shows the calculated value using the Heikes formula. The dashed curve represents the calculated value from the modified Heikes formula, with the orbital degeneracy factor $S = k_B/e[\ln(1-x)/x] + k_B/e[\ln(9/4)]$.

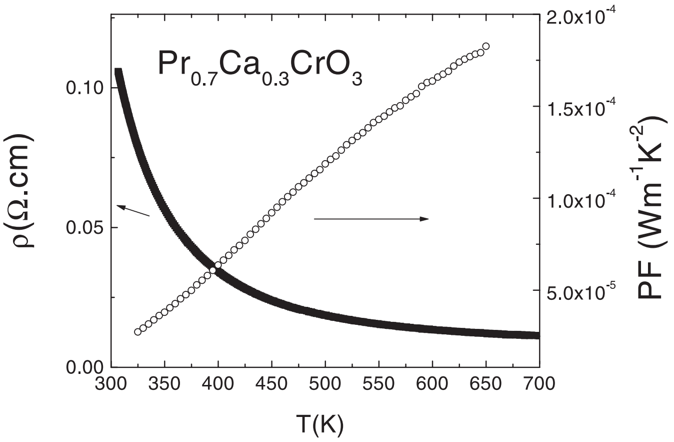

Fig. 6. ρ vs. T (left scale) and Power Factor ($PF = S^2/\rho$) (right scale) of $Pr_{0.7}Ca_{0.3}CrO_3$ measured up to 700 K.

4 Conclusion

Magnetic and transport properties of ceramics $Pr_{1-x}Ca_xCrO_3$ (x = 0.0–0.5) crystallizing in an orthorhombic perovskite structure have been investigated. Magnetic ordering temperature (T_N) reflecting the Cr^{3+}-O-Cr^{3+} superexchange decreases with increase of Ca^{2+} doping. Concomitantly, large decrease in resistivity and Seebeck coefficient (S) are observed as Cr^{4+} is created in the Cr^{3+} matrix by the Ca^{2+} for Pr^{3+} substitution.

Furthermore, the S values are found to be T-independent for the experimental T range (up to ∼700 K). It is found that this Cr^{4+} dependent S values at room temperature follow a modified Heikes formula taking into account the spin and orbital degeneracy responsible for a shift of +69.9 μV/K. The estimated power factor $PF = S^2/\rho$ of the $Pr_{0.7}Ca_{0.3}CrO_3$ orthorhombic perovskite shows promising values for using these orthochromites as p-type elements in thermoelectric applications operating in air at $T \gg 300$ K. This study shows that choosing the correct combination of spin and orbital is crucial to optimize the figure of merit of oxides.

The authors thank Yannick Klein and Sébastien Lemonnier for their help in high temperature measurements.

References

1. P.M. Chaikin, G. Beni, Phys. Rev. B **13**, 647 (1976)
2. A. Oguri, S. Maekawa, Phys. Rev. B **41**, 6977 (1990)
3. D.B. Marsh, P.E. Perris, Phys. Rev. B **54**, 7720 (1996); D.B. Marsh, P.E. Perris, Phys. Rev. B **54**, 16602 (1996)
4. G. Palsson, G. Kotliar, Phys. Rev. Lett. **80**, 4775 (1998)
5. J. Merino, R.H. McKenzie, Phys. Rev. B **61**, 7996 (2000)
6. R.R Heikes, R.W Ure Jr., *Thermoelectricity: Science and Engineering* (Interscience Bublishers, New York-London, 1961)
7. W. Koshibae, S. Maekawa, Phys. Rev. Lett. **87**, 236603 (2001)
8. J.P. Doumerc, J. Solid State Chem. **110**, 419 (1994)
9. N.Q. Minh, J. Am. Ceram. Soc. **76**, 563 (1993)
10. J. Rodrigues-Carvajal, Physica B **192**, 55 (1993)
11. S. Geller, Acta Cryst. **10**, 243 (1957)
12. R.D. Shannon, Acta Cryst. A **32**, 751 (1976)
13. D.P. Karim, A.T. Aldred, Phys. Rev. B **20**, 2255 (1979)
14. J.D. Gordon, R.M. Horneich, S. Shtrikman, B.M. Wanklyn, Phys. Rev. B **13**, 3012 (1976)
15. K. Yoshii, A. Nakamura, J. Solid State Chemistry **155**, 447 (2000)
16. *Oxide thermoelectrics*, Research Signpost, edited by Kunihito Koumoto (2002)
17. K. Fujita, T. Mochida, K. Nakamura, Jpn J. Appl. Phys. **40**, 4644 (2001)